Spin-wave edge modes in finite arrays of dipolarly coupled magnetic nanopillars

Ivan Lisenkov*
Department of Physics, Oakland University, 2200 N. Squirrel Rd., Rochester, Michigan 48309-4401, USA and Kotelnikov Institute of Radio-engineering and Electronics of RAS, 11-7 Mokhovaya St., Moscow 125009, Russia

Vasyl Tyberkevych and Andrei Slavin
Department of Physics, Oakland University, 2200 N. Squirrel Rd., Rochester, Michigan 48309-4401, USA

Pavel Bondarenko and Boris A. Ivanov
Institute of Magnetism, National Academy of Sciences, Kiev, Ukraine and Taras Shevchenko National University of Kiev, 03127 Kiev, Ukraine

Elena Bankowski and Thomas Meitzler
U.S. Army TARDEC, Warren, Michigan 48397, USA

Sergey Nikitov
Kotelnikov Institute of Radio-engineering and Electronics of RAS, 11-7 Mokhovaya St., Moscow 125009, Russia; Moscow Institute of Physics and Technology, 9 Instituskij per., Dolgoprudny, 141700, Moscow Region, Russia; and Saratov State University, 112 Bol'shaya Kazach'ya, Saratov 410012, Russia

(Received 21 July 2014; revised manuscript received 1 September 2014; published 22 September 2014)

The frequency spectrum of spin-wave edge modes localized near the boundaries of a finite array of dipolarly coupled magnetic nanopillars is calculated theoretically. Two mechanisms of edge mode formation are revealed: inhomogeneity of the internal static magnetic field existing near the array boundaries and time-reversal symmetry breaking of the dipole-dipole interaction. The latter mechanism is analogous to the formation mechanism of a surface Damon-Eschbach mode in continuous in-plane magnetized magnetic films and is responsible for the nonreciprocity of edge modes in finite-width nanopillar arrays. The number of edge modes in nanopillar arrays depends on the spatial profile of the internal static magnetic field near the array boundaries and several edge modes are formed if a substantial field inhomogeneity extends over several rows of nanopillars.

DOI: 10.1103/PhysRevB.90.104417 PACS number(s): 75.30.Ds, 75.75.Jn, 75.78.Cd

I. INTRODUCTION

Spin-wave edge modes localized at the system boundaries exist in different types of magnetic systems and are often used in microwave signal processing. A prominent example of a localized spin-wave edge mode is the so-called Damon-Eshbach (DE) magnetostatic wave [1] propagating perpendicular to the direction of a bias magnetic field in an in-plane magnetized magnetic film. The principal mechanism responsible for the formation of the DE edge (or surface) spin-wave mode is the time-reversal symmetry breaking of the dipole-dipole interaction [1,2].

Another example of the spin-wave edge modes are the localized modes formed near the edges of nonellipsoidal magnetic elements [3,4]. The mechanism of formation of these modes is related to the inhomogeneity of the internal static magnetic field existing near the edges of magnetized magnetic elements of a nonellipsoidal shape leading to the creation of effective potential wells where the edge modes are localized. Obviously, edge modes can exist not only in continuous magnetic objects, but also in different types of artificial magnetic periodic structures, or magnonic crystals, e.g., in dipolarly coupled arrays of magnetic elements.

Recently, a new type of topologically protected localized spin-wave mode has been proposed [5,6]. The existence of this new type of mode is supported by the topological properties of the frequency pass bands in the spin-wave spectrum of an artificial magnonic crystal formed by iron inclusions in a matrix formed by an yttrium-iron garnet film [5]. Although the idea of topologically protected spin-wave modes is interesting and original, the practical realization of the proposed structure [5,6] is questionable. Therefore, it is important to study the possibility of formation of edge spin-wave modes in simpler magnetic periodic structures that can be easily fabricated.

The aim of our current work is the theoretical study of the existence and properties of collective spin-wave edge modes that may exist in finite and semi-infinite arrays of magnetic nanopillars, which can be fabricated by the modern methods of electron-beam lithography. These arrays are the artificial magnetic materials (or magnonic crystals) with properties that can be tailored by changing the geometric and/or the magnetic parameters of the array elements by varying the type and sizes of the array lattice, and by applying an external bias magnetic field [7–10]. Moreover, the magnetic properties of such arrays can be changed dynamically by applying pulsed bias magnetic fields of a particular direction, which switch the array from one stable magnetic configuration to another [11]. Such tunability of nanopillar arrays and magnonic crystals make them promising as dynamically reconfigurable materials for future use in magnonic signal processing devices

*ivan.lisenkov@phystech.edu

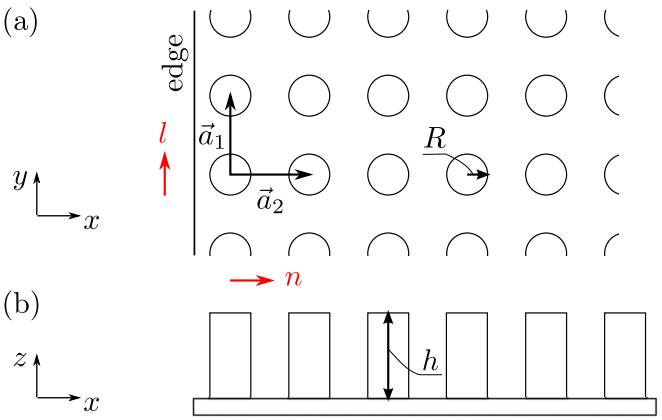

FIG. 1. (Color online) A sketch demonstrating a semi-infinite array of nanopillars with the edge parallel to the primitive lattice vector $\boldsymbol{a}_1$: (a) top view, (b) side view. l and n are the integer pillar indices in the directions parallel and perpendicular to the array's edge, respectively.

[12], e.g., logic devices [13], nonvolatile memory [14], filters, and waveguides [15] operating in the GHz frequency range.

In this paper we present a mathematical formalism to calculate the spectrum and spatial profiles of the spin-wave edge modes in arrays of identical magnetic nanopillars having a simple primitive cell. Using this formalism we demonstrate the existence of edge (or surface) modes and elucidate the physical mechanisms responsible for the formation of these modes. These mechanisms are twofold: (i) the spatial inhomogeneity of the internal static magnetic field existing near the boundaries of the array and (ii) the time-reversal symmetry breaking of the dipolar interaction between the nanopillars forming the array. We also demonstrate that the number of edge modes depends on the spatial profile of the internal static magnetic field near the array boundaries: when the field variation extends over several rows of nanopillars, several edge modes are formed.

II. MATHEMATICAL MODEL

In the macrospin approximation, the dynamics of a magnetization vector $\boldsymbol{M}_i$ of the ith magnetic nanopillar in the array (see Fig. 1) can be described by the Landau-Lifshitz equation [9,16]:

$$d\boldsymbol{M}_i/dt = \gamma\left(\boldsymbol{B}_i^{\mathrm{e}} \times \boldsymbol{M}_i\right), \tag{1}$$

where $\gamma \approx 2\pi \times 28$ GHz/T is the modulus of the gyromagnetic ratio and $\boldsymbol{B}_i^{\mathrm{e}}$ is the effective magnetic field acting on each nanopillar. This field consists of an external magnetic field $\boldsymbol{B}_i^{\mathrm{ext}}$ and a mutual demagnetizing field between the ith and jth magnetic nanopillars:

$$\boldsymbol{B}_i^{\mathrm{e}} = \boldsymbol{B}_i^{\mathrm{ext}} - \mu_0 M_s \sum_j \hat{\boldsymbol{N}}_{ij}(\boldsymbol{r}_i - \boldsymbol{r}_j) \cdot \boldsymbol{M}_j. \tag{2}$$

Here $\hat{\boldsymbol{N}}_{ij}$ is the mutual demagnetizing tensor between the pillars with indices i and j and $\boldsymbol{r}_i$ is the position vector of the ith pillar.

In the case of a sufficiently small precession angle one can decompose the magnetization vector of a nanopillar into the static ($\boldsymbol{\mu}_i$) and dynamic ($\boldsymbol{m}_i$) components: $\boldsymbol{M}_i = M_s(\boldsymbol{\mu}_i + \boldsymbol{m}_i)$ where the following conditions hold: $|\boldsymbol{\mu}_i| = 1$ and $\boldsymbol{\mu} \cdot \boldsymbol{m} = 0$. Using this decomposition one can linearize (1) and split it into two equations, for static and dynamic parts of the magnetization:

$$B_i \boldsymbol{\mu}_i = \boldsymbol{B}_i^{\mathrm{ext}} - \mu_0 M_s \sum_j \hat{\boldsymbol{N}}_{ij} \cdot \boldsymbol{\mu}_j, \tag{3}$$

$$d\boldsymbol{m}_i/dt = \boldsymbol{\mu}_i \times \sum_j \hat{\boldsymbol{\Omega}}_{ij} \cdot \boldsymbol{m}_j, \tag{4}$$

where

$$\hat{\boldsymbol{\Omega}}_{ij} = \gamma B_i \delta_{ij} \hat{\boldsymbol{I}} + \gamma \mu_0 M_s \hat{\boldsymbol{N}}_{ij}(\boldsymbol{r}_i - \boldsymbol{r}_j), \tag{5}$$

B_i is the modulus of the effective static internal magnetic field acting on the ith nanopillar, and $\hat{\boldsymbol{I}}$ is the identity matrix.

Here we shall consider a semi-infinite array of identical nanopillars with an edge that is parallel to one of the high symmetry directions of the array's lattice. In this case we can choose one of the primitive lattice vectors ($\boldsymbol{a}_1$) to be parallel to the array edge (see Fig. 1) and write the position vector $\boldsymbol{r}_i$ as

$$\boldsymbol{r}_i = \boldsymbol{r}_{(n,l)} = l\boldsymbol{a}_1 + n\boldsymbol{a}_2, \tag{6}$$

where l and n are the integer pillar's indices in the directions parallel and perpendicular to the array's edge, respectively, and $\boldsymbol{a}_1$, $\boldsymbol{a}_2$ are the primitive lattice vectors along these directions.

Due to translational symmetry of the array along the $\boldsymbol{a}_1$ direction, the static configuration of the magnetization depends only on the perpendicular n index, $\boldsymbol{\mu}_i = \boldsymbol{\mu}_{(n,l)} = \boldsymbol{\mu}_n$, $B_i = B_{(n,l)} = B_n$, and elementary spin-wave solutions $\boldsymbol{m}_i(t)$ can be found in the form

$$\boldsymbol{m}_i = \boldsymbol{m}_{(n,l)} = \boldsymbol{m}_n e^{ika_1 l - i\omega t}, \tag{7}$$

where k and ω are the wave number and the frequency of the spin-wave mode, respectively. Using these expressions in (4) one can obtain a one-dimensional equation for the spin-wave profile $\boldsymbol{m}_n$:

$$-i\omega \boldsymbol{m}_n = \boldsymbol{\mu}_n \times \sum_{n'} \hat{\boldsymbol{\Omega}}_{k,nn'} \cdot \boldsymbol{m}_{n'}, \tag{8}$$

where

$$\hat{\boldsymbol{\Omega}}_{k,nn'} = \gamma B_n \delta_{nn'} \hat{\boldsymbol{I}} + \gamma \mu_0 M_s \hat{\boldsymbol{E}}_k(n - n'), \tag{9}$$

and

$$\hat{\boldsymbol{E}}_k(n) = \sum_l \hat{\boldsymbol{N}}(l\boldsymbol{a}_1 + n\boldsymbol{a}_2) \cdot e^{-ika_1 l}. \tag{10}$$

Analogously, the static Eq. (3) can be rewritten as:

$$B_n \boldsymbol{\mu}_n = \boldsymbol{B}^{\mathrm{ext}} - \mu_0 M_s \sum_{n'} \hat{\boldsymbol{E}}_0(n - n') \cdot \boldsymbol{\mu}_{n'}. \tag{11}$$

Diagonalization of Eq. (8) yields the dispersion relation for the collective spin waves edge modes in a nanopillar array with an edge. Below we consider only the case of a square array lattice ($|\boldsymbol{a}_1| = |\boldsymbol{a}_2|$ and $\boldsymbol{a}_1 \cdot \boldsymbol{a}_2 = 0$), but the presented

formalism remains valid for any lattice geometry as long as the edge is parallel to one of primitive vectors of the lattice.

III. RESULTS AND DISCUSSION

In our numerical example, instead of a semi-infinite array with one edge, Fig. 1, we considered a finite-width stripe of a square nanopillar array with the lattice constant $a = 4.1R$ having two edges. This stripe had $N = 31$ nanopillars along its width, and the nanopillars in the array were circular cylinders of the radius R and the height $h = 5R$. The static part of magnetization of all the nanopillars was aligned along the same direction parallel to the cylinders' axes, while the external magnetic field was absent [8,9]. The parameters of the array were chosen to guarantee vertical (out of array's plane) anisotropy ($h > R$) of individual nanopillars and sufficient dipolar interaction between the nanopillars ($a < h$) to guarantee formation of collective spin-wave modes in the array. The particular values of these parameters were chosen the same as in Ref. [9] to simplify comparison with the results obtained there.

The results of the numerical calculation of the frequency spectrum of spin-wave modes in such a stripe array are presented in Fig. 2(a). For comparison, the spectrum of the bulk spin-wave modes calculated for an infinite array of nanopillars with the same geometrical parameters using the formalism developed by Verba *et al.* [9] is shown in the same figure by yellow color. It is clear from Fig. 2(a) that several distinct edge modes are seen in the spectrum of the stripe above the spectrum of the bulk modes. The spatial distribution of the time-averaged amplitude of magnetization $\langle m_i \rangle_t = \sqrt{\boldsymbol{m}_i^* \cdot \boldsymbol{m}_i}$ in the four edge modes (with frequencies separated from the bulk spectrum) are shown in Fig. 2(b). It is clear that these modes are strongly localized near the edges of the stripe. The amplitudes of the edge modes almost vanish at the distance of several lattice constants from the edge of the array. Therefore the interaction of modes traveling along the opposite edges of the stripe is negligible for the stripe with $N = 31$ rows.

The main mechanism responsible for the formation of these edge modes is related to the spatial inhomogeneity of the static internal magnetic field near the edges of the stripe [see Fig. 2(c)]. The effect of formation of the edge modes of this kind is typical for nonellipsoidal magnetic samples and has been extensively studied previously [3,17]. Moreover, a similar mechanism of mode localization in a potential well is responsible for the formation of edge states (also known as Tamm states) in other systems of quasiparticles (electrons, photons, phonons, etc.) [18,19]. Since the spatial profile of a static internal magnetic field is symmetric near both edges of the stripe, one would expect that the edge modes would form symmetric pairs, with one edge mode propagating along the left edge of the stripe array and the other one along the right edge. The edge modes, indeed, form split pairs localized near the opposite edges of the stripe. However, the spatial profiles of the modes in each pair are not completely identical, and their dispersion relations are also slightly different [see Figs. 2(a) and 2(b)].

This weak asymmetry of the edge modes propagating along the opposite edges of the stripe is caused by the

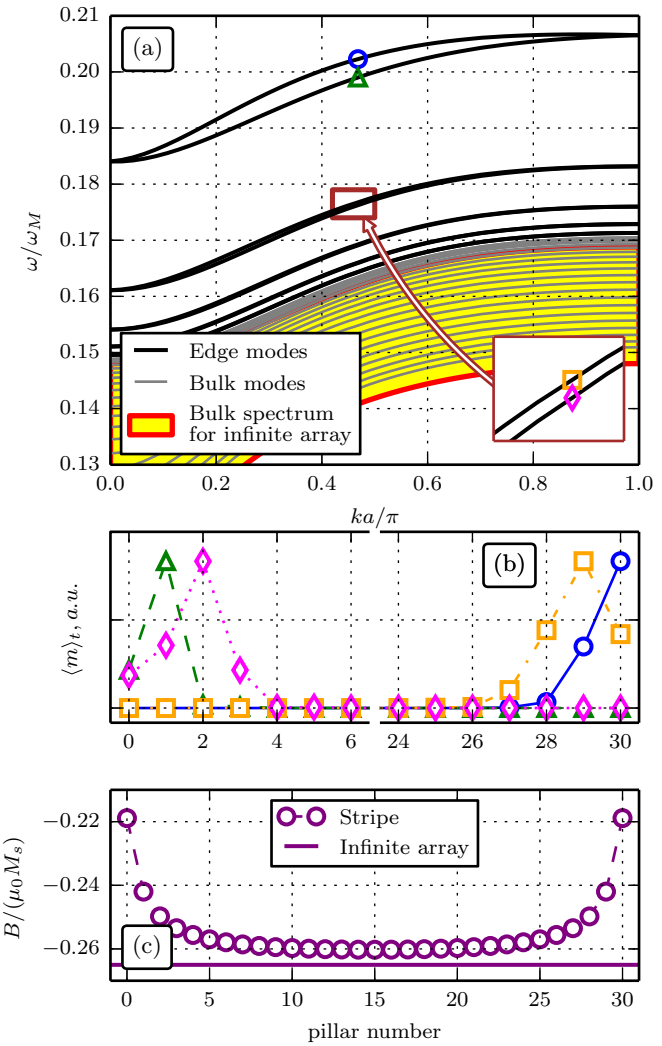

FIG. 2. (Color online) (a) Frequency spectrum of the collective spin-wave modes in a finite-width stripe of dipolarly coupled magnetic nanopillars. The number of nanopilars along the width direction of the stripe (which is parallel to the lattice vector a_2) is equal to $N = 31$. Thick black lines correspond to the edge modes, while thin gray lines correspond to the bulk modes. Yellow region shows the spectrum of bulk modes in an infinitely wide array of nanopillars with the same geometric parameters. (b) Distribution of the time-averaged amplitude of magnetization across the stripe width for the first four edge modes. Corresponding modes are marked by the similar symbols in (a). (c) Distribution of the internal static magnetic field across the stripe width. Parameters of the array: lattice constant $a = 4.1R$, pillar aspect ratio $h/R = 5$.

symmetry-breaking part of the dynamic dipole-dipole interaction with respect to the inversion of the direction of the edge mode propagation (time-reversal symmetry breaking). In particular, this symmetry breaking is responsible for the surface (edge) localization of the DE magnetostatic wave in continuous in-plane magnetized magnetic films [1], and so the DE wave is localized near only one boundary of a film, depending on the travel direction of the wave. Otherwise the boundary conditions at the film edges cannot be satisfied. In our case of nanopillars with perpendicular shape anisotropy the formal origin of the symmetry breaking is the following

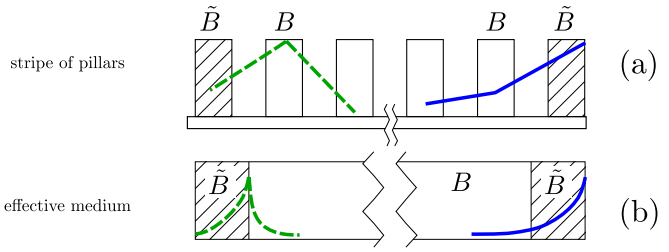

FIG. 3. (Color online) A sketch demonstrating formation of edge modes at the external (solid blue line) and internal (dashed green line) boundaries of a nanopillar stripe. (a) A stripe of magnetic pillars with edge pillars experiencing different internal static magnetic field than the pillars in the bulk. (b) Equivalent effective medium consisting of three continuous magnetic films with different parameters. Damon-Eshbach-like edge modes always form at one side (left side in the figure) of the boundaries (external or internal). This results in the nonreciprocity of edge mode profiles localized near the opposite edges of the stripe.

property of the tensor $\hat{\boldsymbol{E}}_k(n)$ for $n \neq 0$:

$$\hat{\boldsymbol{E}}_k(n) \neq \hat{\boldsymbol{E}}_{-k}(n). \tag{12}$$

This property makes the opposite sides of the stripe not completely equivalent for the edge mode propagation in a particular direction.

In the case of a finite stripe of nanopillars, the static internal magnetic field is nonuniform across the stripe width, thus forming internal boundaries—the rows of nanopillars for which the value of the effective static magnetic field is different from the value in the adjacent row [see Fig. 3(a)]. Thus, the first edge mode in the pair (blue circles in Fig. 2 and Fig. 3), which is localized near the right edge of the stripe, is formed to the left of the external stripe boundary. The second mode (green triangles in Fig. 2 and Fig. 3) is also formed to the left of the boundary, but, in this case, the boundary is internal. This explains why the amplitude maximum of the first edge mode is located at the outermost row of the pillars, while the second mode has the maximum at the second row [see Fig. 2(b)]. A similar situation exists in a continuous magnetic film having spatially nonuniform static magnetization (or internal magnetic field), see Fig. 3(b). So the internal boundaries are formed near the film edges, providing conditions for two nonsymmetric edge modes to exist.

The third and the fourth edge modes in Fig. 2 demonstrate a similar nonsymmetric behavior, but they are localized at the nanopillar rows situated deeper inside the stripe. The number of the formed edge mode pairs depends on the profile of the internal magnetic field and, in the case when the internal field reaches its bulk value on the distance of only 1–2 rows of nanopillars, only one pair of edge modes is formed.

Similar to the DE mode existing in continuous magnetic films, the edge spin-wave modes in a nanopillar stripe, formed near a certain boundary (either external or internal), are nonreciprocal. Due to the rotational symmetry of the problem, the reversal of the direction of a mode propagation moves the mode traveling near the right edge of the stripe to the left edge and vice versa [note that $\hat{\boldsymbol{E}}_k(n) = \hat{\boldsymbol{E}}_{-k}(-n)$]. Also, it is important to note that the frequency splitting in each pair of the

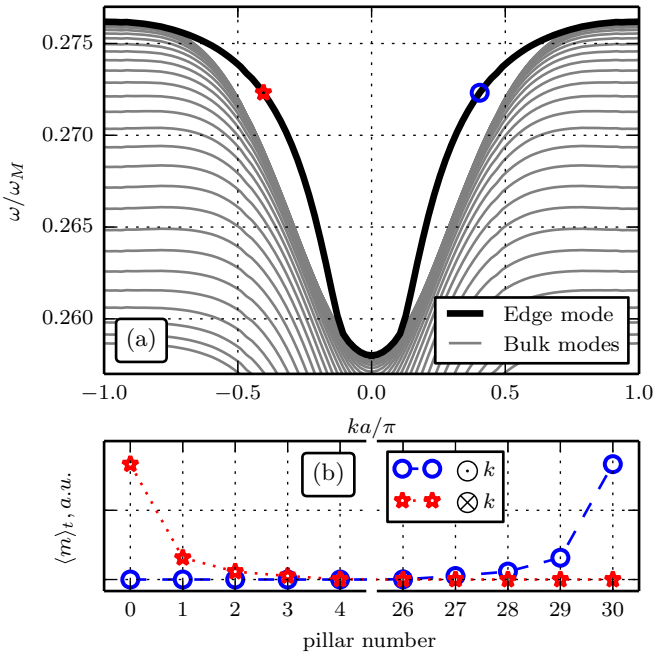

FIG. 4. (Color online) (a) Frequency spectrum of spin-wave modes in a finite-width stripe of magnetic nanopillars with spatially uniform profile of the internal static magnetic field. The black line shows the edge mode, while the gray lines show the bulk modes. (b) Distribution of time-averaged amplitude of magnetization across the stripe width for the edge modes (star and circle symbols denote the edge modes propagating in opposite directions). The array parameters are the same as in Fig. 2, but $h/R = 20$.

edge modes vanishes at the Brillouin zone boundaries (points where $k = 0$ and $k = \pi/a$) as the nondiagonal components of the tensor $\hat{\boldsymbol{E}}_k$, responsible for the nonequality in (12), are also vanishing at these points. For the same reasons both the edge modes frequency splitting and their nonreciprocity exist only in the nanopillar arrays where the magnetizations of the nanopillar elements have an out-of-plane component that leads to the appearance of the nondiagonal components of the tensor $\hat{\boldsymbol{E}}_k$ in the final eigenvalue problem (8).

To study in detail the effects caused exclusively by the symmetry-breaking part of the dipole-dipole interaction we investigated the spin-wave spectrum in an array where the internal static magnetic field was artificially made completely spatially uniform and equal to the internal static magnetic field in an infinite array of nanopillars having the same parameters [see Fig. 4(a)]. The calculations in this artificial uniform field case were performed for the same parameters of the nanopillar array, but using a substantially larger height of the nanopillars $h = 20R$ to increase the dipole-dipole interaction between the nanopillars. In this case only one edge mode is formed, and this mode is localized near either the left or the right outer edge of the array, depending on the direction of the mode propagation [Fig. 4(b)], similar to the DE wave in continuous films.

If the pillars are significantly higher than the width of the array stripe, the problem of the spin-wave dispersion in a stripe is similar to the problem of a magnetostatic wave dispersion in a continuous ferromagnetic film. In this limiting case we can assume the pillars to be infinitely long [16], and the

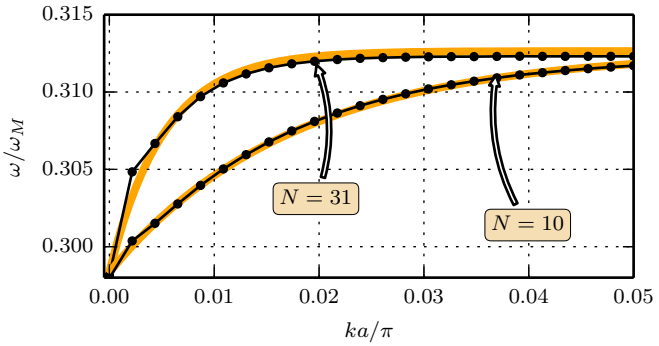

FIG. 5. (Color online) Dispersion of the spin-wave edge modes in two finite-width stripes (with $N = 10$ and $N = 31$ nanopillars along the stripe width) of infinitely high nanopillars (black dots). For comparison, the dispersion of the Damon-Eshbach mode propagating in a continuous magnetic film with equivalent parameters is shown (yellow lines).

dispersion of the edge spin-wave mode can be approximated by the magnetostatic DE dispersion in an effective continuous magnetic film [1,2]:

$$\omega = \sqrt{\omega_0\left(\omega_0 + \omega_M^{\text{eff}}\right) + \frac{\left(\omega_M^{\text{eff}}\right)^2}{4}\left(1 - e^{-2kd}\right)}, \qquad (13)$$

where ω_0 is the FMR frequency in an infinite array of pillars [9], $\omega_M^{\text{eff}} = (\pi R^2/a^2)\omega_M$ characterizes the effective static magnetization of the array [9], and $d = (N-1)a$ is the thickness of the effective magnetic film.

The results of calculations of the spin-wave dispersion for two finite-width stripe arrays with different number of nanopillars ($N = 31$ and $N = 10$) along the stripe width are presented in Fig. 5. The dispersion of the edge modes of the array coincides with the dispersion of the DE wave of the effective magnetic film in the region $ka \ll 1$, where the continuous media approximation holds. Also, in contrast to the previous cases, the dispersion of the edge mode is dependent on the width of the stripe due the long-range character of the dipole-dipole interaction.

IV. CONCLUSIONS

In conclusion, we presented a theoretical formalism that allows one to calculate the collective spin-wave edge modes in semi-infinite and finite arrays of dipolarly coupled magnetic nanopillars. Using this formalism we demonstrated the existence of collective spin-wave edge modes in finite-width stripe arrays of periodically arranged magnetic nanopillars. The edge spin-wave modes are localized at both the outer geometric boundaries of the stripe and at the inner boundaries created due to the spatial inhomogeneity of the static magnetic field near the stripe edges. For arrays of nanopillars having the out-of-plane component of static magnetization the edge modes exhibit nonreciprocal behavior, and their profiles are different for different directions of the wave propagation. The nonreciprocity occurs because of the symmetry-breaking part of dynamic dipole-dipole interaction with respect to the inversion of the propagation direction (t symmetry). The number of the distinct edge modes is determined by the spatial profile of the internal static magnetic field in the stripe, and, for typical nanopillar array parameters, several edge modes with frequencies well separated from the bulk spectrum are formed.

ACKNOWLEDGMENTS

This work was supported in part by the Grant No. DMR-1015175 from the National Science Foundation of the USA, by the contract from the US Army TARDEC, RDECOM, and by the DARPA grant "Coherent Information Transduction between Photons, Magnons, and Electric Charge Carriers". I.L. and S.N. acknowledge the Russian Scientific Foundation, Grant No. 14-19-00760 for financial support.

[1] R. Damon and J. Eshbach, J. Phys. Chem. Solids **19**, 308 (1961).
[2] D. Stancil and A. Prabhakar, *Spin-waves: Theory and Applications* (Springer, London, 2009).
[3] J. Jorzick, S. O. Demokritov, B. Hillebrands, M. Bailleul, C. Fermon, K. Y. Guslienko, A. N. Slavin, D. V. Berkov, and N. L. Gorn, Phys. Rev. Lett. **88**, 047204 (2002).
[4] G. Gubbiotti, M. Conti, G. Carlotti, P. Candeloro, E. D. Fabrizio, K. Y. Guslienko, A. Andre, C. Bayer, and A. N. Slavin, J. Phys.: Condens. Matter **16**, 7709 (2004).
[5] R. Shindou, R. Matsumoto, S. Murakami, and J.-i. Ohe, Phys. Rev. B **87**, 174427 (2013).
[6] R. Shindou, J.-i. Ohe, R. Matsumoto, S. Murakami, and E. Saitoh, Phys. Rev. B **87**, 174402 (2013).
[7] P. V. Bondarenko, A. Yu. Galkin, B. A. Ivanov, and C. E. Zaspel, Phys. Rev. B **81**, 224415 (2010).
[8] P. V. Bondarenko, A. Y. Galkin, and B. A. Ivanov, J. Exp. Theor. Phys. **112**, 986 (2011).
[9] R. Verba, G. Melkov, V. Tiberkevich, and A. Slavin, Phys. Rev. B **85**, 014427 (2012).
[10] R. Verba, V. Tiberkevich, E. Bankowski, T. Meitzler, G. Melkov, and A. Slavin, Appl. Phys. Lett. **103**, 082407 (2013).
[11] R. Verba, V. Tiberkevich, K. Guslienko, G. Melkov, and A. Slavin, Phys. Rev. B **87**, 134419 (2013).
[12] S. Demokritov and A. Slavin, *Magnonics: From Fundamentals to Applications*, *Topics in Applied Physics* (Springer, Berlin, 2012).
[13] R. Nakatani, H. Nomura, and Y. Endo, J. Phys.: Conf. Ser. **165**, 012030 (2009).
[14] M. Albrecht, G. Hu, A. Moser, O. Hellwig, and B. D. Terris, J. Appl. Phys. **97**, 103910 (2005).
[15] K.-S. Lee, D.-S. Han, and S.-K. Kim, Phys. Rev. Lett. **102**, 127202 (2009).
[16] M. Beleggia, S. Tandon, Y. Zhu, and M. De Graef, J. Magn. Magn. Mater. **278**, 270 (2004).
[17] I. Lisenkov, D. Kalyabin, and S. Nikitov, Appl. Phys. Lett. **103**, 202402 (2013).
[18] L. Brekhovskikh, *Waves in Layered Media*, *Applied mathematics and mechanics* (Academic Press, New York, 1980).
[19] I. M. Lifshits and S. I. Pekar, Usp. Fiz. Nauk. **56**, 531 (1955).